Al-Mn Transition Edge Sensors for Cosmic Microwave Background Polarimeters

D. R. Schmidt, H.-M. Cho, J. Hubmayr, P. Lowell, M. D. Niemack, G. C. O'Neil, J. N. Ullom, K. W. Yoon, K. D. Irwin, W. L. Holzapfel, M. Lueker, E. M. George, and E. Shirokoff

***Abstract*—Superconducting transition edge sensors (TES) require superconducting films with transition temperatures (T_c) and properties that can be tailored to the particular requirements of individual applications. We have been developing Al-Mn films with a tunable T_c. The addition of Mn to Al suppresses T_c, but does not significantly broaden the superconducting density of states of the Al. We can produce films with T_c from below 50 mK to 1.4 K through adjustment of the Mn concentration. Since this is a bulk effect, T_c is not as dependent on precise control of film thickness as in the standard bilayer approach for TESs. We have previously used Al-Mn to fabricate TES sensors for x-ray microcalorimeters targeted for read-out with time division SQUID multiplexing schemes. In this work, we explore the properties of Al-Mn in a regime well suited for frequency division multiplexing. We have also fabricated prototype Al-Mn cosmic microwave background polarimeters for the South Pole Telescope and will show initial measurements of these sensors.**

***Index Terms*—AlMn, polarimeter, transition-edge sensor.**

I. Introduction

VOLTAGE biased superconducting transition edge sensors (TES) [1] provide exquisite performance for bolometric and calorimetric applications [2]. The most important parameters to take into account when choosing a material for the superconductor are the transition temperature, T_c, and the normal state resistance of the TES, R_n. The base temperature of the instrument determines T_c, or alternatively desired performance characteristics set T_c, and this choice drives the refrigeration technology. TESs have proven useful over a broad temperature span (10 mK to a few K). The TES is employed on a wide range of low-temperature refrigeration technologies including the dilution refrigerator (DR), adiabatic demagnetization refrigerator (ADR), $^3\mathrm{He}$ refrigerator, and $^4\mathrm{He}$ refrigerator. The type of multiplexing circuitry drives the choice of R_n. A TES operated in the transition has a resistance R_{TES} that is some fraction of R_n. The electrical bandwidth, Δf, must be sufficiently high to maintain feedback stability [3]. The bandwidth also must be rolled off to limit performance degradation from white (Johnson) noise and to reduce the overall bandwidth required to multiplex many sensors.

Time-divison multiplexing (TDM) operates with boxcar modulated baseband signals. A dissipative filter is formed from the R_{TES} and an additional inductance, L, which is typically lithographically patterned on a separate die. The resultant bandwidth of this filter is $\Delta f = R_{TES}/(2\pi L)$. R_{TES} can be chosen to be low ($\approx 5 - 50\ \mathrm{m}\Omega$) and L scales to low values ($\approx$10-500 nH). A lower resistance TES will have better internal thermalization and smaller inductances are simpler to fabricate. Frequency domain multiplexing (FDM) operates with narrow band rf signals. Each pixel has a tuned LC filter with a center frequency given by $f_i = 1/2\pi\sqrt{L_iC_i}$. To keep $0.3 > f_i > 1.0$ MHz, practical considerations drive C_i and L_i to higher values ($L_i \approx 10 - 20\ \mu\mathrm{H}$). The same L both tunes the resonator and controls the bandwidth. Fixing L_i forces R_i higher to maintain the bandwidth $\Delta f_i = R_{TESi}/(2\pi L_i)$. FDM generally operates with a TES R_n range of 0.5 - 2 Ω. While R_n is not strictly a material parameter, the desire to work with superconducting films which are not exceedingly thin ($t \ll 20$ nm) or thick ($t \gg 300$ nm) sets the requirements for the resistivity, ρ, of the film.

The ranges of desired T_c and R_n span a few orders of magnitude, and rarely has nature provided an elemental solution to the choice of superconductor. A common approach employed to tune T_c and R_n is to utilize a bilayer of a superconductor and a normal metal. In a superconducting bilayer the presence of the normal metal will suppress T_c. Adjustment of the thicknesses of both the normal metal and superconductor can provide some control of both T_c and R_n [4]. Another method is to modify a bulk superconductor through doping. Magnetic doping of tungsten TES devices was used to adjust the T_c of sensors for detection of dark matter [5]. The range of T_c adjustment possible with magnetic doping is limited. Magnetic impurities tend to broaden the superconducting peak in the superconducting density of states (DOS); large scale adjustment of the superconducting gap is not possible without significant broadening of the gap edge. There are also non-magnetic impurities that can adjust T_c through manipulation of the conduction band DOS.

One superconductor that is amenable to adjustment of T_c by non-magnetic impurities is Al. The addition of a small Mn content to Al can control the T_c of the Al film from an undoped value of ~1.4 K to below 50 mK [6]. In this process, the transition width remains relatively narrow and the Al-Mn DOS is still Bardeen–Cooper–Schrieffer (BCS) in character [7]. Above T_c, the Al-Mn film can be used like a normal metal.

Manuscript received August 01, 2010; accepted October 11, 2010. Date of publication November 22, 2010; date of current version May 27, 2011.

D. R. Schmidt, H.-M. Cho, J. Hubmayr, P. Lowell, M. D. Niemack, G. C. O'Neil, J. N. Ullom, K. W. Yoon, and K. D. Irwin are with the National Institute of Standards and Technology, Boulder, CO 80305 USA (e-mail: schmidtd@nist.gov).

W. L. Holzapfel, M. Lueker, E. M. George, and E. Shirokoff are with the Physics Department, University of California, Berkeley, CA 94720 USA.

Color versions of one or more of the figures in this paper are available online at http://ieeexplore.ieee.org.

Digital Object Identifier 10.1109/TASC.2010.2090313

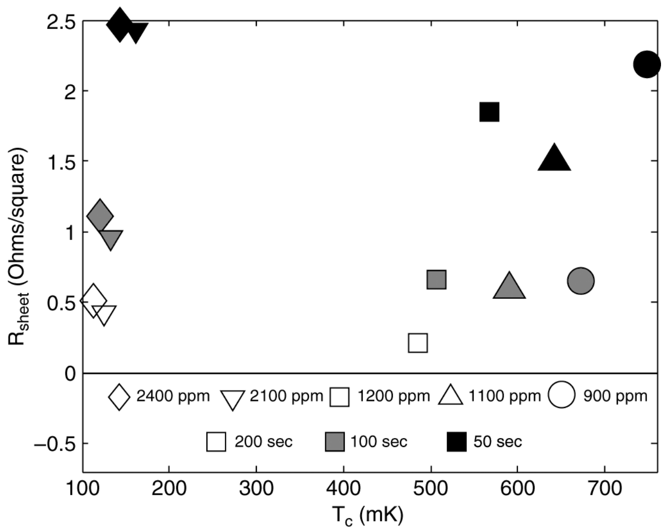

Fig. 1. Al-Mn film characterization. The normal state sheet resistance and transition temperature T_c were measured for films produced with five different Al-Mn sputter targets with different Mn concentrations: (circles) 900 ppm, (upwards facing triangles) 1100 ppm, (squares) 1200 ppm, (downward facing triangles) 2100 ppm, and (diamonds) 2400 ppm. The shading indicates the deposition time: (black) 50 s, (gray) 100 s, and (no shading) 200 s.

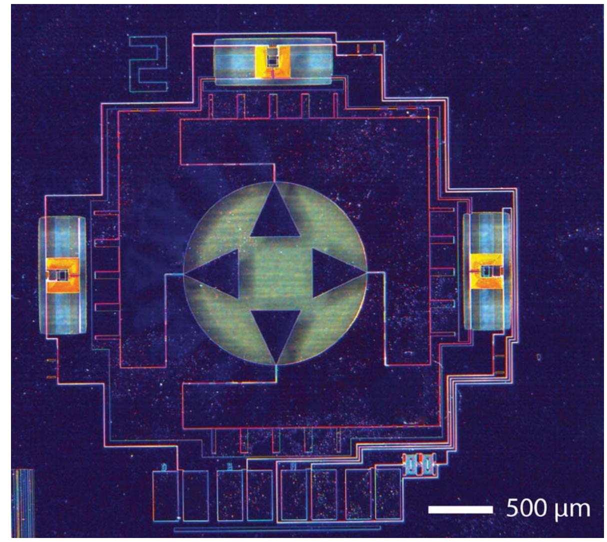

Fig. 2. Optical micrograph of a prototype polarimeter. (Center) The orthomode transducer and a matching circuit couples radiation from a waveguide onto superconducting niobium microstrip where the signals pass through bandpass and low-pass filters to define the band before the signals are terminated on thermally isolated islands. The power deposited into each island is monitored by an Al-Mn TES.

Tunnel junctions made with Al and Al-Mn have been successfully used to form normal metal-insulator-superconductor (NIS) refrigerators [8]. These desirable properties motivated our fabrication of Al-Mn TESs for x-ray microcalorimeters measured with TDM [9]. Unfortunately, since the Al-Mn dilute alloy is inherently resistive, the films required for TDM TES are thick ($t > 400$ nm for $R_n < 100$ mΩ) and internal thermalization of the calorimeter may be hampered. However, the resistivity of the Al-Mn film makes it an appropriate candidate for TES targeted for FDM readout.

In this paper, we investigate the suitability of Al-Mn TES sensors for a polarization sensitive instrument on the South Pole Telescope (SPTpol). SPTpol will have 650 polarimeters operating at 150 GHz and 200 detectors operating at 90 GHz [10]. In this paper we will discuss materials for the 150 GHz polarimeters. The readout technology for SPTPol is FDM, and the focal plane is cooled by a three stage $^4\mathrm{He} - ^3\mathrm{He} - ^3\mathrm{He}$ refrigerator with a base temperature of 300 mK. The target R_n for the detectors is $\approx 1.0\ \Omega$ and the target T_c is ≈550 mK.

II. Characterization of Al-Mn Films

Deposition of Al-Mn is readily accomplished with dc-magnetron sputtering. The vapor pressure discrepancy between Al and Mn makes evaporative methods less desirable. We maintain a dedicated sputter system for Al-Mn films. The system has three guns that accept 7.62 cm (3 in) targets and an ion-mill used for pre-cleaning as necessary. The system can accommodate up to 150 mm substrates. For this study, we had a series of targets fabricated with varying Mn concentration.

We characterized our Al-Mn by depositing films from our target selection in a range of film thicknesses. Parameters common to all depositions are the Ar gas pressure (0.33 Pa, 2.5 mTorr) and the sputter gun power (600 W). The substrates were Si wafers with a 120 nm thermal oxide. The new targets were burned in for an initial duration of 30 min. The average deposition rate was ∼0.45 nm/s with little deviation between the targets. Half of each wafer was wet etch patterned into $10\ \mu\mathrm{m} \times 100\ \mu\mathrm{m}$ strips for 4-wire resistance measurements. The whole wafer was diced into 6 mm × 6 mm die.

Transition temperature measurements were done on the unpatterned die in an ADR. Sheet resistance measurements were done at 4 K in a liquid helium probe on the patterned die. Fig. 1 shows the results from a characterization run of five different Al-Mn sputter targets. The three lower Mn concentration films (900, 1100, and 1200 ppm by atomic%) have T_c between 450 and 750 mK and are potentially suitable for operation at a 300 mK base temperature. The higher concentration films (2100 and 2400 ppm by atomic %) have T_c between 100 and 200 mK; these films would be suitable for TESs mounted on an ADR or DR. For a deposition duration of 100 s (film thickness ≈45 nm) the lower Mn concentration films have a sheet resistance of $\sim 0.7\ \Omega$ per square. In this regime, there is a thickness dependence to T_c. If the thickness uniformity across the wafer is better than 5%, the resultant T_c variation from this effect is less than 1 mK. As a sputter target wears, the deposition rate will have to be periodically calibrated to precisely track the desired T_c.

III. Prototype Polarimeters

Using the previously described characterization as a guide we proceeded to fabricate prototype polarimeters. Fig. 2 shows an optical micrograph of a polarimeter test pixel. An orthomode transducer and a matching circuit couple microwave power incident from a feed horn into two TESs through niobium microstrip. The microstrips terminate in lossy meanders located on suspended silicon nitride islands. Fig. 3 shows an optical micrograph of a suspended island. At the center of the island is an Al-Mn TES. Contacts made from Nb define the active area of the TES to be $48\ \mu\mathrm{m} \times 68\ \mu\mathrm{m}$. In the first fabrication run a 45

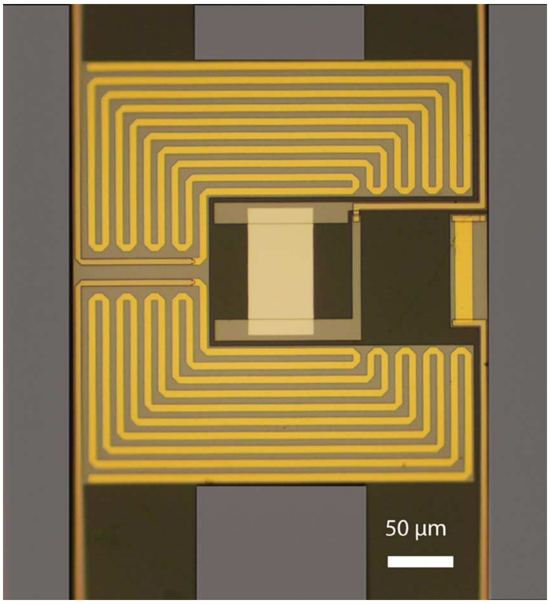

Fig. 3. Optical micrograph of TES island. Structurally, the island is made from suspended silicon nitride supported by four legs. At the center of the island is an Al-Mn TES ($48\ \mu\mathrm{m} \times 68\ \mu\mathrm{m}$) contacted by Nb leads that enter the island as microstrip the top right leg of the island. To the right of the TES is a Au strip heater with corresponding lead entering the island via the bottom right leg. The TES is surrounded by two separate Au meander line terminations. The leads for the meanders come in from the top left and bottom left. The terminations couple power from the orthomode transducer, as shown in Fig. 2, to the TES island.

nm thick Al-Mn film (1200 ppm Mn) was used. The measured R_n and T_c were $\sim 0.9\ \Omega$ and ~540 mK. Right of the TES is a Au strip to apply dc heat to the island. The polarimeter layout is a variant of a design we have previously used with Mo:Cu bilayer TESs [11].

The prototype polarimeters were tested in a refrigerator at 250 mK. In general the Al-Mn TESs displayed typical TES characteristics. However the onset of electro-thermal oscillations deep in the transition $(R < 0.7R_N)$ indicates that the heat capacity of the island is too small. Currently we are fabricating Al-Mn TESs with additional heat capacity designed to stabilize the detectors. One method we are using is known as bandwidth limiting interface normally gold (BLING) [12]. We are also investigating use of thicker Al-Mn patterned into a meander to preserve the desired value of R_n.

References

[1] K. D. Irwin, *Appl. Phys. Lett.*, vol. 66, p. 1998, 1995.

[2] K. D. Irwin and G. C. Hilton, "Transition-edge sensors," in *Cryogenic Particle Detection, Topics Appl. Phys*, C. Enss, Ed. Heidelberg, Germany: Springer-Verlag Press, 2005, vol. 99, pp. 63–149.

[3] K. D. Irwin, G. C. Hilton, D. A. Wollman, and J. M. Martinis, *J. Appl. Phys.*, vol. 83, p. 3978, 1998.

[4] K. D. Irwin, G. C. Hilton, J. M. Martinis, S. Deiker, N. Bergren, S. W. Nam, D. A. Rudman, and D. A. Wollman, *Nucl. Instrum. Meth. Phys. Res. A*, vol. 444, p. 184, 2000.

[5] B. A. Young, T. Saab, B. Cabrera, J. J. Cross, and R. A. Abusaidi, *Nucl. Instrum. Meth. Phys. Res. A*, vol. 444, p. 428, 2000.

[6] G. O'Neil, D. Schmidt, N. A. Miller, J. N. Ullom, A. Williams, G. B. Arnold, and S. T. Ruggiero, *Phys. Rev. Lett.*, vol. 100, p. 056804, 2008.

[7] G. C. O'Neil, D. R. Schmidt, N. A. Tomlin, and J. N. Ullom, *J. Appl. Phys.*, vol. 107, p. 093903, 2010.

[8] A. M. Clark, A. Williams, S. T. Ruggiero, M. L. van den Berg, and J. N. Ullom, *Appl. Phys. Lett.*, vol. 84, p. 625, 2004.

[9] S. W. Deiker, W. Doriese, G. C. Hilton, K. D. Irwin, W. H. Rippard, J. N. Ullom, L. R. Vale, S. T. Ruggiero, A. Williams, and B. A. Young, *Appl. Phys. Lett.*, vol. 85, p. 2137, 2004.

[10] J. J. McMahon, K. A. Aird, B. A. Benson, L. E. Bleem, J. Britton, J. E. Carlstrom, C. L. Chang, H. S. Cho, T. de Haan, T. M. Crawford, A. T. Crites, A. Datesman, M. A. Dobbs, W. Everett, N. W. Halverson, G. P. Holder, W. L. Holzapfel, D. Hrubes, K. D. Irwin, M. Joy, R. Keisler, T. M. Lanting, A. T. Lee, E. M. Leitch, A. Loehr, M. Lueker, J. Mehl, S. S. Meyer, J. J. Mohr, T. E. Montroy, M. D. Niemack, C. C. Ngeow, V. Novosad, S. Padin, T. Plagge, C. Pryke, C. Reichardt, J. E. Ruhl, K. K. Schaffer, L. Shaw, E. Shirokoff, H. G. Spieler, B. Stadler, A. A. Stark, Z. Staniszewski, K. Vanderlinde, J. D. Vieira, G. Wang, R. Williamson, V. Yefremenko, K. W. Yoon, O. Zhan, and A. Zenteno, "Low temperature detectors LTD 13," in *Proc. 13th Int. Workshop on Low Temperature Detectors* , 2009, vol. 511.

[11] K. W. Yoon, J. W. Appel, J. E. Austermann, J. A. Beall, D. Becker, B. A. Benson, L. E. Bleem, J. Britton, C. L. Chang, J. E. Carlstrom, H.-M. Cho, A. T. Crites, T. Essinger-Hileman, W. Everett, N. W. Halverson, J. W. Henning, G. C. Hilton, K. D. Irwin, J. McMahon, J. Mehl, S. S. Meyer, S. Moseley, M. D. Niemack, L. P. Parker, S. M. Simon, S. T. Staggs, K. U-yen, C. Visnjic, E. Wollack, and Y. Zhao, "Low temperature detectors LTD 13," in *Proc. 13th Int. Workshop on Low Temperature Detectors* , 2009, vol. 515.

[12] E. Shirokoff, B. A. Benson, L. E. Bleem, C. L. Chang, H. Cho, A. T. Crites, M. A. Dobbs, W. L. Holzapfel, T. Lanting, A. T. Lee, M. Lueker, J. Mehl, T. Plagge, H. G. Spieler, and J. D. Vieira, *IEEE Trans. Appl. Supercond.*, vol. 19, p. 517, 2009.